Measuring the Binodal by Interdiffusion in Blends of Deuterated Polystyrene and Poly(styrene-*co*-4-bromostyrene)

F. Bruder* and R. Brenn

Fakultät für Physik, Universität Freiburg, D-7800 Freiburg, Germany

Received December 5, 1990; Revised Manuscript Received May 17, 1991

ABSTRACT: Via interdiffusion of the two pure components we measured the binodals of blends of deuterated polystyrene (dPS) and poly(styrene-*co*-4-bromostyrene) (PBr_xS) with elastic recoil detection (ERD). We varied the molecular weights of the components and the degree of bromination x of the copolymer. The data are analyzed within the Flory–Huggins description for a blend of a homopolymer and a statistical copolymer. In the case of a very asymmetric blend we measured the shift of the interface during the equilibration of the bilayer to two-phase coexistence. For short diffusion times we find the time behavior predicted by a simple step model for the concentration dependence of the diffusion coefficient over a miscibility gap.

Introduction

In recent years several methods have been developed that have sufficient depth resolution to measure the concentration profile at polymer–polymer interfaces and polymer surfaces. Methods that are working in direct space are elastic recoil detection (ERD),[1,2] secondary ion mass spectrometry (SIMS),[3–6] and nuclear reaction analysis (NRA).[7,8] In Fourier space most of the published work has been done by neutron and X-ray reflectivity methods.[6,9,10] Early work dealt with miscible polymer–polymer blends, whereas now more and more interest is spent on interfaces of partially miscible blends and surfaces of polymer blends to vacuum. Chaturvedi et al.[7] measured the interfacial width of a high molecular weight blend of deuterated polystyrene (dPS) and polystyrene (PS) with a nuclear reaction method. Anastasiadis et al.[9] investigated the interface of PS–PMMA block copolymers with neutron reflection, applying X-ray reflection to monitor the total sample thickness. Fernandez et al.[10] studied the interface of the respective homopolymers. Also Jones et al.[6] used neutron reflection and secondary ion mass spectrometry to study the surface composition of a blend of dPS and PS.

Up to now all these data are interpreted in terms of mean-field theories. Therefore an essential parameter of the blend that has to be known is the Flory–Huggins interaction parameter, χ. Blends of deuterated polystyrene and poly(styrene-*co*-4-bromostyrene) should be interesting systems, which also provide good contrast for all the measurement methods mentioned above: ERD, SIMS, NRA, X-ray, and neutron reflection. Compatibility in this blend can be controlled by the degree of bromination x of the copolymer and by the molecular weights of the two components. By a suitable choice of these parameters the upper critical solution temperature of this blend lies well above its glass transition temperature and below the region where thermal degradation sets in. Also a possible lower critical solution temperature expected due to different thermal expansion coefficients of the monomer units[11] should lie above the temperature for thermal degradation in the blends used in this study. While the blend of PS and PBr_xS was already well characterized by Strobl and co-workers[12] (measurements of the χ parameter and the Kuhn segment length in the dependence of both the degree of bromination and the blend composition), we reported in an earlier paper[13] about measurements of the χ parameter of blends of dPS and PBr_xS. They showed an enhancement of χ due to the deuteration of the homopolymer. While in this early work we were able to measure only one of the compositions on the coexistence curve, we now succeeded to measure both due to another choice of thickness of the initial bilayer of the two components. Binodals were extracted from the data for three different blends at two different degrees of bromination. We then try to express the effective interaction parameter by the mutual interaction parameters between pairs of the respective segments involved in these blends.

Using a simple model for interdiffusion in a blend with a miscibility gap, we are able to verify experimentally the predicted time dependence of the shift of the interface for short diffusion times during equilibration toward two-phase coexistence.

Experimental Section

All polymers in this work were purchased from Polymer Standards Service[14] (see Table I). The bromination of the polystyrene was carried out following a procedure described elsewhere.[15] The degree of bromination x was computed from the mass densities, which were measured by a suspension method and a calibration table of mass density versus degree of bromination x.[12] Blends obtained from bilayers of these polymers are labeled in the following manner (see Table I): blend 1 = polymer A and polymer D, blend 2 = polymer B and polymer D, blend 3 = polymer C and polymer E. Diffusion couples of blend 2 and blend 3 were formed by first spinning a solution of the copolymer in chloroform onto a polished silicon wafer. This gives about 300–500-nm-thick films after drying. Then films of dPS of about 250–350-nm thickness were spun onto a glass slide, floated off onto the surface of distilled water, and picked up onto a substrate consisting of the copolymer film on the silicon wafer. Bilayers of blend 1 consist of a thick lower film of PBr_xS ($\approx$1–2 μm) and a thinner upper film of dPS ($\approx$200–400 nm). The formation of these couples was described elsewhere.[13] The bilayers were heated in a vacuum oven ($p \leq 10^{-6}$ Torr) above their glass transition temperature up to 60 h. Then they were quenched to ambient temperature at a rate of about 50 K/min so that the concentration profile was frozen in. After this treatment the concentration profile of the deuterated polystyrene was measured with elastic recoil detection.

In this technique[1] a beam of 2.8-MeV $^4He^+$ ions strikes the diffusion couple at a glancing angle (15° from the target plane). The $^4He^+$ ions collide elastically with the target atoms, which are knocked out of the target at forward angles. These recoils are registered by an energy-dispersive surface barrier detector. In this way deuterons obtain a fraction of about 0.66 of the projectile energy compared to a fraction of 0.48 for protons, both observed at a forward angle of 30°. Target atoms ejected from deeper layers of the target have lower energies due to the energy loss of the incident ions and the recoils on their way through the target material. With a table of stopping powers for the particles involved[22] the energy difference between recoils from the surface

0024-9297/91/2224-5552$02.50/0

Table I[a]

polymer	label	M_w	M_w/M_n	x	N
dPS	A	129 700	1.02		1158
dPS	B	123 000	1.05		1098
dPS	C	640 000	1.07		5714
PBr_xS	D	130 000	1.03	0.1190	1285
PBr_xS	E	170 000	1.05	0.0617	1660

[a] x denotes the degree of bromination. Typical relative error for x of the suspension method is <1%. M_w denotes the weight-average molecular weight before bromination of the polystyrene.

and recoils from deeper layers in the target can be converted to a depth scale for each hydrogen isotope in the target. Also the height of the energy spectrum can be converted to a concentration scale using the known cross section for the scattering process.[16] In practice the measured energy spectrum of an unknown dPS profile is divided by a spectrum of a pure dPS target measured under the same conditions. A 10-μm-thick mylar foil is placed in front of the detector to prevent elastically scattered $^4He^+$ projectiles from reaching it, so that only deuterons and protons are registered. The depth resolution near the surface is about 85 nm and is caused mainly by energy straggling of the recoils in the mylar foil. The maximum depth for which the dPS profile can be measured is about 750 nm. This depth limit results from the overlap of the energy spectra of deuterons coming from this depth and protons kicked out from the target surface. To register the total beam dose on the target, a metal cylinder with appropriate windows for beam transport and detectors was set around the target. A dc voltage of −400 V relative to the scattering chamber and the target suppresses secondary electrons ejected out of the target, so that a beam integrator gives a reproducible measure of the total beam dose. In addition, a surface barrier detector was mounted at 90° scattering angle as a second normalization instrument. It monitors the energy spectra of projectiles scattered from C and Si atoms in the target and backing. Because dPS and PBr_xS have the same concentration of C, these spectra can also be used in normalization. Typical normalization errors are about 7%. To keep beam damage in the sample low, the target was shifted to a new position, with respect to the beam, for several times after a total dose of about 3.3-μC $^4He^+$. The beam current was kept at about 4 nA. The respective energy spectra gathered from the different spots on one target were added in the computer to enhance count rate statistics. PBr_xS being very sensitive to radiation damage, the Br profile, measured by Rutherford backscattering spectroscopy (RBS) of a pure sample of PBr_xS, changed appreciably during data collection. We observed a depletion of Br increasing toward the surface of the sample. This depletion is ascribed to the loss of highly mobile HBr. This depletion is reduced if the target is cooled, e.g., to the temperature of a mixture of alcohol and CO_2. The observed deuterium profiles of the diffusion couples remained the same with the targets cooled or not. So if there is also a deuterium loss during data collection it should be homogenous in depth. Also the loss of Br does not affect the depth scale significantly via a possible dependence of the net stopping power on the target composition, because the degree of bromination is low and therefore Br has no significant contribution to the stopping power. The simulated deuteron yield in a matrix of pure PBr_xS with $x = 0.119$ compared to that in a matrix of pure PS differs only up to 0.3%. All ERD measurements were carried out at the 7.5-MeV Van de Graaff accelerator of the University of Freiburg, Germany.

Results and Discussion

(A) Binodals and χ Parameters. In this section we want to discuss the measurement of the binodals for the blends and the computation of their Flory–Huggins interaction parameters for different molecular weights and different degrees of bromination x of the copolymer. We first refer to the measurements of blend 2 and blend 3 carried out for similar conditions and then give a recalibrated set of data for blend 1, which were obtained with a different initial thickness of the bilayers compared to blend 2 and blend 3.

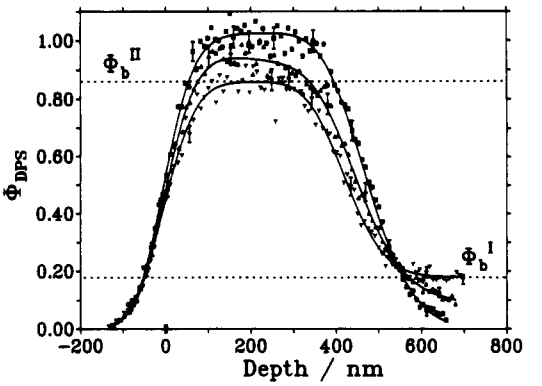

Figure 1. Interdiffusion profiles of a bilayer of blend 2. The total layer thickness is about 1000 nm, and the diffusion temperature is 197 °C. Profiles are recorded after diffusion times of 0.0 (■), 804 (▲), and 18 990 s (Y). Extracted values of the compositions at the binodal are $\Phi_b^{II} = 0.86$ and $\Phi_b^{I} = 0.18$. The error bars at every 10th point of the profiles are calculated from count rate statistics of the respective energy spectra.

Bilayers of the pure components were used as described previously. The dPS film was on top and the PBr_xS film beneath. Each film had a thickness of about 300–500 nm. After interdiffusion at a temperature above the glass transition temperature region of the blend and for a sufficiently long time a bilayer of the two coexisting phases of the blend is expected to establish, with the dPS-rich phase at the surface. One has to carefully choose the relative thicknesses of the two films so that, especially in the asymmetric blend, e.g., blend 3, the mean composition does not lie in the one-phase region at the actual diffusion temperature. If this should be the case, no bilayer will establish for long diffusion times; instead a film of homogenous composition (the mean composition) will develop. Figure 1 shows concentration profiles as an illustration example of interdiffusion going on in blend 2. Error bars were calculated from count rate statistics of the respective energy spectra. From the initial bilayer of the two pure components a bilayer of the two coexisting phases has developed. The interface did not show any further broadening during the interdiffusion besides the width caused by the finite depth resolution. The real thickness of the interface could not be measured with ERD because of the poor depth resolution of about 100 nm at the interface. This observed degradation of depth resolution at the interface compared to the surface arises mainly from thickness variations of the top dPS layer. Energy straggling in the target down to the depth of the interface would produce a much smaller effect.

Before we describe the extraction of the compositions of the coexisting phases from the data, we want to discuss interdiffusion in a blend with a miscibility gap in terms of a steplike concentration dependence of the interdiffusion coefficient. In what follows, sub- or superscripts II (I) always denote properties on the dPS-rich (-poor) side of the couple. The compositions (volume fractions of dPS) of the coexisting phases are labeled Φ_b^{II} and Φ_b^{I}. Then we define a mean diffusion coefficient D_I in the concentration regime $0 \le \Phi \le \Phi_b^{I}$ on the dPS-poor side of the miscibility gap and a mean diffusion coefficient D_{II} in the concentration regime $\Phi_b^{II} \le \Phi \le 1$ on the dPS-rich side of the gap. The interface is modeled as a step in the concentration profile going from Φ_b^{II} to Φ_b^{I}. The initial conditions ($t = 0$) are $\Phi = 1$ for $z \le R_0$ and $\Phi = 0$ for $z \ge R_0$ where R_0 denotes the initial position of the interface. For $t \ge 0$ the diffusion equation must be solved separately

on both sides of the interface

$$\frac{\partial \Phi^i}{\partial t} = D_i \frac{\partial^2 \Phi^i}{\partial z^2} \tag{1}$$

with i = I for $z \geq R(t)$ and i = II for $z \leq R(t)$. $R(t)$ denotes the position of the interface for $t \geq 0$. At the interface the solution has to obey the boundary conditions

$$\Phi^i(R,t) = \Phi_b{}^i \tag{2}$$

and because the diffusing substance must be conserved

$$\frac{dR}{dt}(\Phi_b{}^{II} - \Phi_b{}^{I}) = D_I \frac{\partial \Phi^I}{\partial z}(R,t) - D_{II} \frac{\partial \Phi^{II}}{\partial z}(R,t) \tag{3}$$

This problem can be solved in a straightforward manner[17] for an infinitely extended diffusion couple.

$$\Phi^{II}(z,t) = 1 - \gamma \operatorname{erfc}\left(\frac{R_0 - z}{(4D_{II}t)^{1/2}}\right) \tag{4a}$$

$$\Phi^{I}(z,t) = \alpha \operatorname{erfc}\left(\frac{z - R_0}{(4D_{I}t)^{1/2}}\right) \tag{4b}$$

$$R(t) = R_0 + \delta\sqrt{t} \tag{5}$$

The three constants α, γ, and δ are determined by the three boundary conditions at the interface. The solution of this model (eqs 4 and 5) should describe the experimental situation as long as the volume fractions at the surfaces of a finite diffusion couple differ only slightly from their initial values.

The composition of the coexisting phases was extracted from the data in the following way. If there was left a measurable concentration gradient to the left and to the right of the interface, we used a fitting function adopted from the diffusion model proposed above. The solution of this model can be replaced by a step function of heights $\Phi_b{}^I$ and $\Phi_b{}^{II}$ for diffusion times of sufficient duration. This function was convoluted with a Gaussian of a fwhm of 85 nm at the surface and a fwhm of 100 nm at the interface. For higher temperatures and lower molecular weights interdiffusion was so fast that the step function was always a good approximation. For blend 3 (the blend with the high molecular weight dPS) the mean values obtained from the fits for the two longest diffusion times were taken as $\Phi_b{}^I$ and $\Phi_b{}^{II}$. Parts a and b of Figure 2 show the pairs of points $\Phi_b{}^I$ and $\Phi_b{}^{II}$ on the binodals of blend 2 (○) and blend 3 (■), obtained by the procedure described above. It is worth mentioning that there is good agreement with the critical volume fraction $\Phi_c = 1/(1 + \sqrt{r})$ of 0.52 for blend 2 (symmetric) and 0.35 for blend 3 (asymmetric) where r denotes the ratio of the polymer molar volumes of dPS and PBr_xS. The measured binodals show clearly the appropriate symmetry or asymmetry expected for blends with equal or unequal polymer molar volumes of the components. To compute Φ_c, the differing specific volumes in the glassy state were taken into account to estimate the ratio r of the polymer molar volumes. Assuming volume additivity, this can be done by using the mass densities of the components given, for example, in ref 12. The effective degrees of polymerization relative to the molar volume of a styrene unit are also given in Table I.

To complete the discussion, we now refer to our former measurements of blend 1.[13] These have been carried out with a different oven, and a recalibration of its requires a correction of the temperature. Because of the now

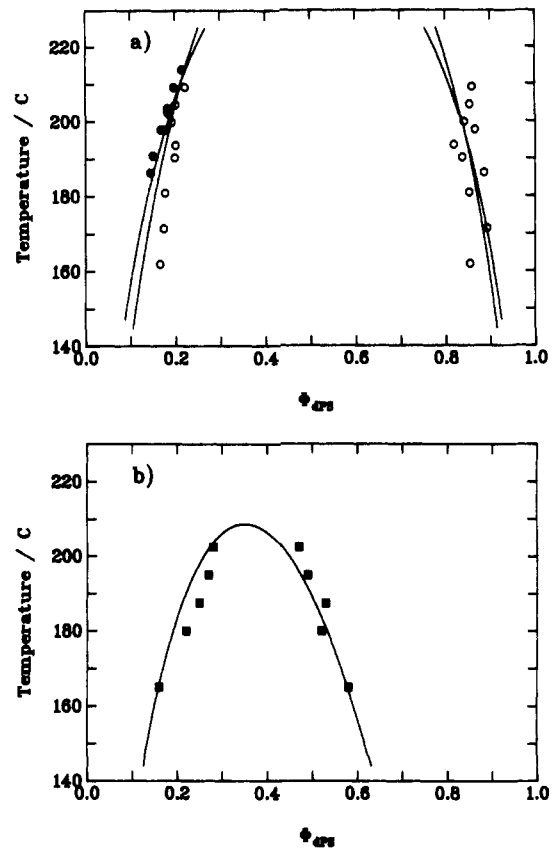

Figure 2. (a) Binodals of blend 1 (●) and blend 2 (○). The data of blend 1 have been recalibrated relative to the previous paper.[13] $\Phi_b{}^{II}$ are the points on the dPS-rich side and $\Phi_b{}^I$ are points on the dPS-poor side of the miscibility gap. Blend 2 shows a somewhat weaker temperature dependence and a higher T_c than blend 1. (b) Binodal of blend 3 (■).

improved normalization procedure used for blend 2 and blend 3, a slight correction of the composition data is also necessary. In these earlier measurements thinner films of dPS (200–400 nm) lie on top of thick films of PBr_xS (1–2 μm). In these measurements we could only extract one of the two compositions ($\Phi_b{}^I$) from the profiles. Because of the much larger thickness of the PBr_xS layer relative to the dPS layer, the mean composition of the diffusion couple was usually in the one-phase region, so that the interface could not be sustained in some cases for the longest diffusion times. In most cases the remaining layer of the dPS-rich phase was so thin after finite diffusion times that within the depth resolution of ERD no plateau could be measured in the profile. So in ref 13 we used a fitting function that kept the concentration of dPS constant at 100% in the dPS-rich phase. In the dPS-poor phase an exponential decay with $\Phi_b{}^I$ at the position of the interface was used. Details are discussed in ref 13. Figure 2a shows the data, recalibrated in temperature and composition (●), of blend 1. From the old values $\varphi_b{}^I$ and $\varphi_b{}^{II} = 1$ we rescaled to the new values with $\Phi_b{}^I + \Phi_b{}^{II} = 1$, keeping the ratios $\Phi_b{}^{II}/\Phi_b{}^I = \varphi_b{}^{II}/\varphi_b{}^I$. This should be a reasonable procedure because this blend is almost symmetric. The data show a slightly higher T_c for blend 2 than for blend 1 arising from a somewhat weaker curvature of the binodal in blend 2 than in blend 1, whereas the $\Phi_b{}^I$ of blend 1 lie above the $\Phi_b{}^I$ of blend 2 in most cases, as expected due to the slightly higher molecular weight of the dPS used in blend 1. This discrepancy can arise from the different analysis procedures and initial conditions used for both blends (different fit functions). Because of the thick PBr_xS films in blend 1, equilibrium was never reached during the diffusion times in our old measurements.

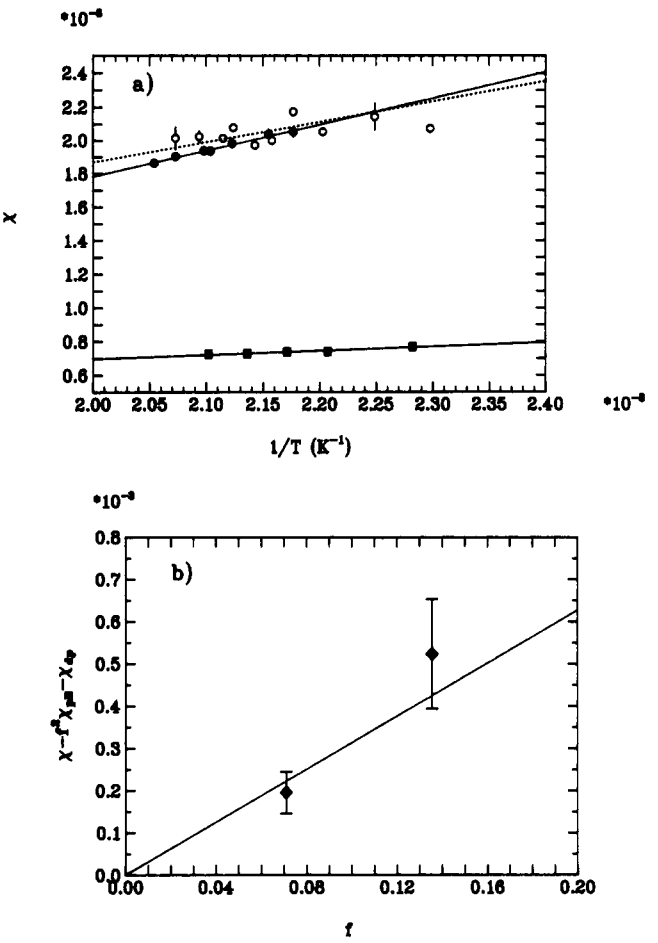

Figure 3. (a) Flory–Huggins interaction parameter χ versus $1/T$ for degrees of bromination $x = 0.1190$ (blend 1 (●) and blend 2 (○)) and $x = 0.0617$ (blend 3 (■)). (b) $f(\chi_{dB} - \chi_{dp} - \chi_{pB}) = \chi - f^2\chi_{pB} - \chi_{dp}$ plotted versus the degree of bromination expressed in volume fraction $f(x)$. The values are taken at 180 °C. Error bars are computed by error propagation assuming a 6% error for χ and a 2.6% error for χ_{pB}. χ_{dB} was extracted from the slope of the linear least-squares fit.

Table II[a]

blend	A/K	B
dPS/PS[b]	0.20 ± 0.01	$-(2.9 \pm 0.4) \times 10^{-4}$
dPS/PS[c]	0.22 ± 0.06	$-(3.2 \pm 1.2) \times 10^{-4}$
PS/PBrS[d]	20.9	0.032
blend 1	1.57 ± 0.08	$-(1.36 \pm 0.16) \times 10^{-3}$
blend 2	1.22 ± 0.89	$-(0.57 \pm 1.87) \times 10^{-3}$
blend 3	0.25 ± 0.03	$+(1.94 \pm 0.06) \times 10^{-4}$

[a] $\chi = A/T + B$, the parameters A and B are measured in the temperature range of 140–210 °C. T is the absolute temperature in Kelvin. [b] Reference 18. [c] Reference 19. [d] Reference 12, the measured values of χ are scaled to a degree of bromination $x = 1$ by $\chi = f^2\chi_{pB}$.

From the measured binodals the Flory–Huggins interaction parameter χ was calculated, neglecting a possible composition dependence of χ. The procedure, using the common tangent construction, is described in the appendix. Figure 3a shows χ plotted versus the reciprocal of the absolute temperature. We found the expected linear behavior of χ with the reciprocal absolute temperature $1/T$. The straight lines are fits to the data. The fitting parameters are listed in Table II. They are only used to calculate χ values in the temperature region under consideration and not to extrapolate χ to higher or lower temperatures. Also listed are the parameters for blends of dPS/PS[18,19] and PS/PBr$_x$S.[12] The stronger curvature of the binodal of blend 1 compared to blend 2 is also reflected in a stronger temperature dependence of χ. However, the values of χ in the common temperature region only differ up to 5%.

Following the suggestion of ten Brinke, Karasz, and McKnight[20] and Paul and Barlow,[21] the interaction parameter χ of a homopolymer and a statistical copolymer is expressed as

$$\chi = f\chi_{dB} + (1-f)\chi_{dp} - f(1-f)\chi_{pB} \quad (6)$$

where the subscripts denote the interacting pairs of segments: p = protonated styrene, d = deuterated styrene, and B = brominated styrene in the 4-position. f denotes the volume fraction of the brominated styrene units in the random copolymer. f was calculated from the degree of bromination x with the mass densities given in ref 12:

$$f = x\frac{1}{x + (1-x)0.862} \quad (7)$$

0.862 is the ratio of the molar volumes of a styrene and a brominated styrene unit. Figure 3b shows a linearization of eq 6.

$$(\chi - f^2\chi_{pB} - \chi_{dP}) = (\chi_{dB} - \chi_{dP} - \chi_{pB})f \quad (8)$$

The positive slope of this plot indicates a χ_{dB} larger than χ_{pB} even larger than $\chi_{pB} + \chi_{dP}$. Fitting the data using χ_{dP}, χ_{pB}, and χ as calculated from the parameters of Table II gives a value of $\chi_{dB} = 0.081 \pm 0.002$ as compared to that of $\chi_{pB} = 0.078 \pm 0.002$ at $T = 180$ °C, for example. Hence, within the error bars, this difference is not significant.

(B) Interface Shift. In this second section we discuss the interface shift occurring during the evolution of the bilayer of the two pure phases to a bilayer of the two coexisting phases by interdiffusion. The interface shift is expected to be very pronounced in the case of an asymmetric blend, if we start with films of equal thicknesses. In blend 3 $\Phi_b^{I} + \Phi_b^{II} < 1$, and so, if the initial thickness $h = R(t=0)$ of the dPS layer is about half the total thickness L of the bilayer, the final thickness $R_f = R(t\to\infty)$ of the dPS-rich phase will be given by

$$R_f\Phi_b^{II} + (L - R_f)\Phi_b^{I} = h = L/2 \quad (9)$$

with $R_f > L/2$. So the interface has to move in space during the equilibration. Figure 4a shows the profiles of bilayers of blend 3 after various diffusion times for a temperature of 165 °C. The total thicknesses of the bilayers were smaller than 750 nm so that the initial thickness h of the dPS layer could be obtained by simply integrating the profile. We found that the thickness h of the dPS layer could be reproduced within ±50 nm from film to film with the applied spin-casting procedure. The same holds for the thickness of the PBr$_x$S layer. The difference between the actual interface position $R(t)$ and the initial thickness h gives the interface shift for the actual diffusion time. These results are plotted in Figure 4b for temperatures of $T = 180$ °C and $T = 165$ °C. The faster diffusion at the higher temperature and the relaxation to a constant shift at long diffusion times are obvious, whereas for $T = 165$ °C the equilibrium position was not reached yet. Before equilibrium is reached the interface shift is, in good approximation, proportional to the square root of the diffusion time.

For a finite diffusion couple the solutions (eqs 4a,b and 5) of our diffusion model should only hold for a short enough diffusion time, i.e., as long as the compositions at the boundaries of the bilayer have not changed appreciably from their initial values. Nevertheless, we found the $\sqrt{t}$ behavior for times when this is no more the case. So it seems that finite size effects do not have a strong influence

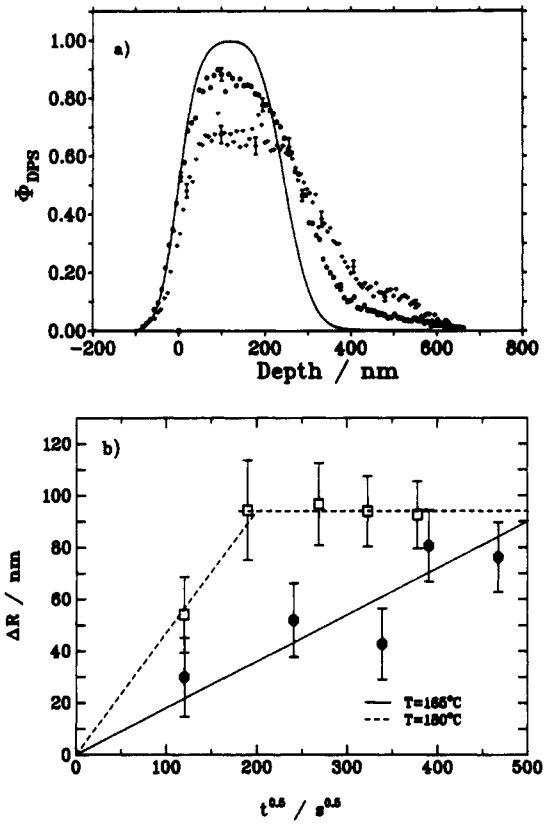

Figure 4. (a) Diffusion profiles at various diffusion times for blend 3 at 165 °C. Two profiles were chosen with almost the same initial thickness h of the dPS layer. The solid line represents the undiffused case for h = 250 nm. Diffusion times were 14 460 (●) and 152 460 s (+). (b) Interface shift $\Delta R = R(t) - h$ versus $\sqrt{t}$. Error bars arise from the 7% normalization error for each h value and an error of ±6 nm for the determination of R. Each point in the plot is the mean of two measurements at two different beam positions on the target.

on the interface shift for our conditions up to diffusion times when equilibrium is reached.

From out model we now estimate a diffusion coefficient D from the measured interface shift by inserting eq 4 into eq 3 and setting $D_I = D_{II} = D$ for simplicity. This yields

$$\xi \exp(\xi^2)(1 + \operatorname{erf} \xi) = \frac{1 - (\Phi_b^{II} + \Phi_b^{I})}{\Phi_b^{II} - \Phi_b^{I}}\sqrt{\pi} \qquad (10)$$

$$\xi = \delta/(4D)^{1/2} \qquad (11)$$

For a direct estimation of D by fitting eq 4 to the profiles the sensitivity of the method is too poor, so that we could not get any consistent parameters. Using the measured values of $\delta = 0.47 \pm 0.08$ nm·s$^{-0.5}$ for T = 180 °C and $\delta = 0.18 \pm 0.02$ nm·s$^{-0.5}$ for T = 165 °C and the respective compositions on the binodal at these temperatures, one can solve for D. In this way we get $D(T$=180 °C) = (1.5 ± 0.5) × 10^{-15} cm^2/s and $D(T$=165 °C) = (2.8 ± 0.6) × 10^{-16} cm^2/s. It should be mentioned that finite size effects can play a very important role for the interface shift. For example, one can choose the initial thickness h and the total thickness L in such a way that $h = R_f$. Then for small times the interface moves away from its initial position but will return to it at long diffusion times.

Green et al.[23] measured the interface shift during the interdiffusion of a low molecular weight polystyrene into a high molecular weight polystyrene. The monitored the movement of gold markers located at the initial interface of the bilayer for t = 0 via Rutherford backscattering spectroscopy (RBS). Kramer et al.[24] explained the marker movement toward the low molecular weight polystyrene with bulk flow that compensates the buildup of a density gradient that should occur if the faster moving species (low molecular weight) diffuses in the slower moving species (high molecular weight). His ansatz yields the following expression for the interdiffusion coefficient ("fast" theory) in the one-phase region of an interacting polymer blend

$$D(\Phi) = ((1 - \Phi)N_A D_A^* + \Phi N_B D_B^*)\left(\frac{1 - \Phi}{N_A} + \frac{\Phi}{N_B} - 2\chi(\Phi(1 - \Phi))\right) \qquad (12)$$

D_A^* and D_B^* are the respective tracer diffusion constants of polymer A in polymer B and vice versa. (The labels A and B have nothing to do with the labels in Table I.)

Whether the interface shift in our measurements can be correlated or not to marker movements due to bulk flow in our blend could be decided by a corresponding experiment with gold markers at the initial interface of our diffusion couple. This will be left to future work. Nevertheless, ignoring all effects of the low degree of bromination on D_A^* and D_B^*, we calculated $D(\Phi)$ with the well-known D_A^* and D_B^* for polystyrene[25] at Φ_b^I and Φ_b^{II} at T = 165 °C (label A was identified with the dPS).

$$D(\Phi_b^I) = 2.4 \times 10^{-15}\ \text{cm}^2/\text{s} \quad \text{with } \Phi_b^I = 0.16$$

$$D(\Phi_b^{II}) = 5.4 \times 10^{-15}\ \text{cm}^2/\text{s} \quad \text{with } \Phi_b^{II} = 0.58$$

The discrepancy of these values with our extracted mean diffusion coefficient is up to a factor of 20. In our opinion this discrepancy should be mainly due to the fact that at the spinodal line $D(\Phi)$ goes to zero. In our experiment mass transport takes place over a miscibility gap accompanied by a shift of the interface (the concentration region in the gap). So the measured mean D also includes parts from concentration regimes inside the miscibility gap where the interdiffusion process is slowed down. To our knowledge, this type of interface shift was not observed before.

We conclude with a brief summary. We have shown that interdiffusion in a bilayer can serve as a method to measure the binodal of a partially miscible polymer blend. The Flory–Huggins interaction parameter for a blend of a homopolymer and a statistical copolymer, extracted as a model parameter from the measured binodals, was analyzed according to the ansatz of Paul and Barlow[21] and ten Brinke, Karasz, and McKnight.[20] Within this model we found χ_{dB} about 4% larger than χ_{pB} measured with SAXS.[12] Further we measured the shift of the interface during the evolution of the bilayer to two-phase coexistence. This shift is proportional to the square root of the diffusion time in the early stage of interdiffusion. From this time dependence a mean model diffusion coefficient near the binodal could be estimated.

Acknowledgment. This work was supported by Deutsche Forschungsgemeinschaft (SFB 60). F.B. thanks the Graduiertenkolleg Polymerwissenschaften at the University of Freiburg, Germany. We also thank Uwe Lüttringhaus for his assistance during the long accelerator runs, the operators of the Van de Graaff accelerator at the University of Freiburg, and Prof. G. R. Strobl for helpful discussions.

Appendix

The χ parameter was calculated by the common tangent construction at the excess free enthalpy of mixing g per cell volume Ω, chosen to be the molar volume of a styrene unit.

$$g(\Phi_b^{II}) = g(\Phi_b^{I}) + \Delta\mu(\Phi_b^{II} - \Phi_b^{I}) \tag{A1}$$

$$\Delta\mu = \frac{\partial g}{\partial \Phi}(\Phi_b^{I}) = \frac{\partial g}{\partial \Phi}(\Phi_b^{II}) \tag{A2}$$

and

$$g(\Phi)/(kT) = \frac{\Phi}{N_A}\ln\Phi + \frac{(1-\Phi)}{N_B}\ln(1-\Phi) + \chi\Phi(1-\Phi) \tag{A3}$$

Φ denotes the volume fraction of component A.

Equation A1 combined with eq A2 can be solved for χ as a function of Φ_b^{I} and Φ_b^{II}. The resulting equations will be different when Φ_b^{I} or Φ_b^{II} is inserted in the expression for $\Delta\mu$ but give the same value for χ if the exact Φ_b^{I} and Φ_b^{II} are used.

$$-(\Phi_b^{II} - \Phi_b^{I})^2\chi - \left(\frac{1}{N_A} - \frac{1}{N_B}\right)(\Phi_b^{II} - \Phi_b^{I}) = \frac{1}{N_B}(1-\Phi_b^{I})\ln\left(\frac{1-\Phi_b^{II}}{1-\Phi_b^{I}}\right) + \frac{1}{N_A}\Phi_b^{I}\ln\left(\frac{\Phi_b^{II}}{\Phi_b^{I}}\right) \tag{A4}$$

$$(\Phi_b^{II} - \Phi_b^{I})^2\chi - \left(\frac{1}{N_A} - \frac{1}{N_B}\right)(\Phi_b^{II} - \Phi_b^{I}) = \frac{1}{N_B}(1-\Phi_b^{II})\ln\left(\frac{1-\Phi_b^{II}}{1-\Phi_b^{I}}\right) + \frac{1}{N_A}\Phi_b^{II}\ln\left(\frac{\Phi_b^{II}}{\Phi_b^{I}}\right) \tag{A5}$$

Due to experimental uncertainities in Φ_b^{I} and Φ_b^{II}, this was never the case. However, the extracted values of χ differ less than about 3.5%. We quote the mean of the two values of χ.

Binodals were constructed by first finding pairs of compositions with a common tangent at $g(\Phi)$. This was done by elimination of χ with the help of eqs A4 and A5. The resulting equation was solved for Φ_b^{II} (Φ_b^{I}) with a Newton method. To these pairs was matched the appropriate χ parameter by using eq A1 again.

References and Notes

(1) Mills, P. J.; Green, P. F.; Palmstrom, C. J.; Mayer, J. W.; Kramer, E. J. *Appl. Phys. Lett.* **1984**, *45*, 957.
(2) Jones, R. A. L.; Kramer, E. J.; Rafailovich, M. H.; Sokolov, J.; Schwarz, S. A. *Phys. Rev. Lett.* **1989**, *62*, 280.
(3) Jones, R. A. L.; Kramer, E. J.; Rafailovich, M. H.; Sokolov, J.; Schwarz, S. A. *Mater. Res. Soc. Symp. Proc.* **1989**, *153*, 133.
(4) Whitlow, S. J.; Wool, R. P. *Macromolecules* **1989**, *22*, 2648.
(5) Coulon, G.; Russell, T. P.; Deline, V. R.; Green, P. F. *Macromolecules* **1989**, *22*, 2581.
(6) Jones, R. A. L.; Norton, L. J.; Kramer, E. J.; Composto, R. J.; Stein, R. S.; Russell, T. P.; Mansour, A.; Karim, A.; Felcher, G. P.; Rafailovich, M. H.; Sokolov, J.; Zhao, X.; Schwarz, S. A. *Europhys. Lett.* **1990**, *12*, 41. Jones, R. A. L.; Kramer, E. J.; Ravailovich, M. H.; Sokolov, J.; Schwarz, S. A.; *Mater. Res. Soc. Symp. Proc.* **1989**, *153*, 133.
(7) Chaturvedi, U. K.; Steiner, U.; Zak, O.; Krausch, G.; Klein, J. *Phys. Rev. Lett.* **1989**, *63*, 616. Chaturvedi, U. K.; Steiner, U.; Zak, O.; Krausch, G.; Schatz, G.; Klein, J. *Appl. Phys. Lett.* **1990**, *56*, 1228.
(8) Payne, R. S.; Clough, A. S.; Murphy, P.; Mills, P. J. *Nucl. Instrum. Methods* **1989**, *B42*, 130.
(9) Anastasiadis, S. H.; Russell, T. P.; Satija, S. K.; Majkrzak, C. F. *Phys. Rev. Lett.* **1989**, *62*, 1852. Anastasiadis, S. H.; Russell, T. P.; Satija, S. K.; Majkrzak, C. F. *J. Chem. Phys.* **1990**, *92*, 5677.
(10) Fernandez, M. L.; Higgins, J. S.; Penfold, J.; Ward, R. C.; Shackelton, C.; Walsh, D. J. *Polymer* **1988**, *29*, 1923.
(11) Strobl, G. R.; Bendler, J. T.; Kambour, R. P.; Shultz, A. R. *Macromolecules* **1986**, *19*, 2683.
(12) Strobl, G. R.; Urban, G. *Colloid Polym. Sci.* **1988**, *266*, 398. Koch, T.; Strobl, G. R. *J. Polym. Sci. B* **1990**, *28*, 343.
(13) Bruder, F.; Brenn, R.; Stühn, B.; Strobl, G. R. *Macromolecules* **1989**, *22*, 4434.
(14) Polymer Standards Service, 6500 Mainz, FRG.
(15) Kambour, R. P.; Bendler, J. T. *Macromolecules* **1986**, *19*, 2679.
(16) Nagata, S.; Yamaguchi, S.; Fujino, Y. *Nucl. Instrum. Methods* **1985**, *B6*, 533. Besenbacher, F.; Stensgaard, I.; Vase, P. *Nucl. Instrum. Methods* **1986**, *B15*, 459. Lüttringhaus, U.; Bruder, F.; Brenn, R., to be published.
(17) Crank, J. *The Mathematics of Diffusion*; Oxford University Press: Oxford, U.K., 1975.
(18) Bates, F. S.; Wignall, G. D. *Phys. Rev. Lett.* **1986**, *57*, 1429.
(19) Green, P. F.; Doyle, B. L. *Macromolecules* **1987**, *20*, 2471.
(20) Brinke ten, G.; Karasz, F. E.; McKnight, W. J. *Macromolecules* **1983**, *16*, 1827.
(21) Paul, D. R.; Barlow, J. W. *Polymer* **1984**, *25*, 487.
(22) Ziegler, J. F. *The Stopping and Ranges of Ions in Matter*; Pergamon Press: New York, 1977; Vol. 4. Anderson, H. H.; Ziegler, J. F. *The Stopping and Ranges of Ions in Matter*; Pergamon Press: New York, 1977; Vol. 3.
(23) Green, P. F.; Palmstrom, C. J.; Mayer, J. W.; Kramer, E. J. *Macromolecules* **1985**, *18*, 501.
(24) Kramer, E. J.; Green, P. F.; Palmstrom, C. J. *Polymer* **1984**, *25*, 473.
(25) Green, P. F.; Kramer, E. J. *Macromolecules* **1986**, *19*, 1108.